How to cite: *Angew. Chem. Int. Ed.* **2025**, *64*, e202424952
doi.org/10.1002/anie.202424952

Inorganic Materials

The First Antimony Borosulfates Unveil a Modular System $M^{III}M^{I}[B(SO_4)_2]_4$ ($M^{III} = Bi^{3+}$, Sb^{3+}, Lu^{3+}; $M^{I} = H_3O^+$, NO_2^+, Li^+, Na^+, K^+, Rb^+, Cs^+)

*Erich Turgunbajew and Henning A. Höppe**

Abstract: Recently we reported the synthesis and characterization of $Bi(H_3O)[B(SO_4)_2]_4$, at that time representing only the second tectosilicate analogous borosulfate. Inspired by this structure type, we herein present the first modular system within borosulfate chemistry. $M^{III}M^{I}[B(SO_4)_2]_4$ ($M^{III} = Bi^{3+}$, Sb^{3+}, Lu^{3+}; $M^{I} = H_3O^+$, NO_2^+, Li^+, Na^+, K^+, Rb^+, Cs^+) were synthesised under solvothermal conditions and show a large variability towards their mono- and trivalent cation while retaining the same three-dimensional anionic network. Based on their combination, the titled compounds crystallize in the tetragonal space groups $I\bar{4}$ (no. 82), $P\bar{4}$ (no. 81) and the monoclinic space group $C2$ (no. 5) all connected via group-subgroup relations. Our initial characterization includes single-crystal as well as powder X-ray diffraction, vibrational spectroscopy and thermal analysis of the new compounds.

Silicate-analogous materials play an important role in our daily life as molecular sieves, phosphors, or catalysts.[1] The longest-known group which already has been studied since the mid-1800s, are probably alumosilicates, where aluminium formally replaces silicon partially yielding vertex connected AlO_4 and SiO_4 tetrahedra.[2] Ever since, many variations of the TX_4 basic building unit have been developed with T being P, S, B and X standing for N, O or F.[3] By introducing boron, in addition to BO_4 tetrahedra, trigonal planar BO_3 groups may be established or by replacing oxygen with nitrogen several tetrahedra can be connected by a common corner, both not known in the classic silicate chemistry.[4] This results in an almost infinite range of diversity beyond the already vast variability. Another, rather young class of materials alike alumosilicates are borosulfates.[5] Here, typically borate and sulfate tetrahedra condense via common vertices forming B–O-S bridges. Additionally, unconventional B–O-B and S–O-S connecting motifs as well as trigonal BO_3 units were already found, resulting in an already impressive variability in this system yielding promising compounds for NLO applications, phosphors or proton conduction only naming a few.[6,7]

An approach barely applied in borosulfate chemistry so far is the use of two differently charged cations. A group around Li et al. published a derivative of the nesosilicate analogue borosulfate $Rb_5[B(SO_4)_4]$ formally replacing one Rb atom by the smaller Li atom.[8] This exchange induced a symmetry reduction resulting in the non-centrosymmetric space group $I\bar{4}$ and exhibiting a SHG effect 1.1 times of potassium dihydrogen phosphate (KDP). Additionally, $CsK_4[B(SO_4)_4]$, $Cs_3Na_2[B(SO_4)_4]$, and $Cs_3Li_2[B(SO_4)_4]$ are known applying the same approach, however, all compounds comprise only two cations of the same charge and sharing the same site.[5] Considering the related compound class of borophosphates the approach of using two or more differently charged cation species is more commonly there. $M^{I}_xM^{II}_y[BP_2O_8] \cdot 3H_2O$ with $M^{I}_x = Li^+$, Na^+, K^+, H_3O^+ and $M^{II}_y = Co^{2+}$, Mn^{2+}, Mg^{2+}, Ni^{2+}, Fe^{2+}, Zn^{2+}) comprise vertex connected borate and phosphate tetrahedra resulting in a helical anionic structure with monovalent cations lying within the helices and divalent cations in between, connecting the latter.[9] In 2021, our group reported $Bi(H_3O)[B(SO_4)_2]_4$ at this time only the second tectosilicate analogous structure known as well as being the first borosulfate with two differently charged cations.[10] We present in our contribution the discovery of a modular system which facilitates the synthesis of a manyfold of related compounds by the exchange of mono- and trivalent cations. This contribution gives a concise overview about this highly versatile structure type with systematic variation of space groups and first insights into its materials properties.

Accordingly, with $M^{III}M^{I}[B(SO_4)_2]_4$ ($M^{III} = Bi^{3+}$, Sb^{3+}, Lu^{3+}; $M^{I} = H_3O^+$, NO_2^+, Li^+, Na^+, K^+, Rb^+, Cs^+) we introduce the first modular system with two differently charged cations in borosulfate chemistry.[11] The title compounds were synthesized under solvothermal conditions starting from the respective cation sources - like oxides, carbonates, sulfates and nitrates -, boron oxide and oleum (65 % SO_3) yielding colorless, phase pure crystalline powders. Interestingly, the oleum content may be reduced to a mixture of 1:1 with sulfuric acid ending up with the same result. On the phase diagram BaO-B_2O_3-SO_3, our group demonstrated that by controlling the oleum content, it is possible to selectively obtain S–O–S, B–O–S and B–O–B

[*] M. Sc. E. Turgunbajew, Prof. Dr. H. A. Höppe
Lehrstuhl für Festkörperchemie
Universität Augsburg
Universitätsstr. 1, 86159 Augsburg (Germany)
E-mail: henning.hoeppe@physik.uni-augsburg.de

bridges within the anion's structure.[6d] So far, solely this connection type but not the dimensionality can be controlled. Regarding the dimensionality in the borosulfate chemistry, a general trend becomes obvious: primarily 0D borosulfates form when solely sulfuric is employed, while higher dimensional structures are more probable when oleum or distilled SO_3 is used. A correlation of the dimensionality with SO_3 content is not evident, though. While some syntheses driven with distilled SO_3 yield in 1D chains, herein we present a synthesis with a 1:1 ratio of oleum (65 % SO_3) to sulfuric acid and yield a 3D network. The control of dimensionality remains an open question.

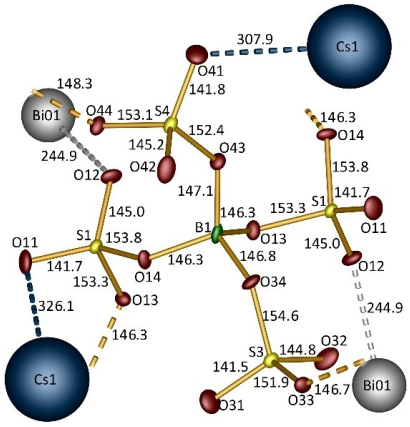

Figure 1. Exemplified $B(SO_4)_4^{5-}$ anion cut-out from $BiCs[B(SO_4)_2]_4$; yellow dotted lines portray the vertex connection of sulphate tetrahedra via all four corners to further boron atoms resulting in the three-dimensional network. O11 and O21 coordinate mono-, O12 and O22 respectively coordinate trivalent cations; boron, green; sulphur, yellow; oxygen, red; ellipsoids are set to 70% probability.

Table 1: Space groups of $M^{III}M^{I}[B(SO_4)_2]_4$ ($M^{III} = Bi^{3+}$, Sb^{3+}, Lu^{3+}; $M^{I} = Li^{+}$, Na^{+}, K^{+}, Rb^{+}, Cs^{+}) compared with ionic radii of M^{I}.[14]

	r(M^{I}) / pm	Bi	Sb	Lu
Li	92	$I\bar{4}$	$I\bar{4}$	$I\bar{4}$
Na	118	$I\bar{4}$	$I\bar{4}$	$I\bar{4}$
K	151	$I\bar{4}$	$C2$	$I\bar{4}$
Rb	160	$P\bar{4}$	$C2$	$P\bar{4}$
Cs	174	$P\bar{4}$	$P\bar{4}$	$P\bar{4}$

According to a B:(SO_4) ratio of 1:2, the borosulfate anion reveals a tectosilicate analogue structure with typical $B(SO_4)_4^{5-}$ basic building units (Figure 1) connected via all four sulfate groups spanning a 3D-framework (Figure 2a). Consequently, two distinct 1D channels along the c-direction are formed, with one channel hosting the singly charged cations and the other containing the triply charged cations. Considering the reduced representation of the basic building unit, BS_4 supertetrahedra, the smaller trivalent cations reside in the channels formed by vierer rings while the larger monovalent cations are found along the channels formed by achter rings (Figure 2b). Based on their respective combination the channels' morphology is modified leading to a change in symmetry, as illustrated in Table 1. This raises the question of the driving forces behind the observed symmetry changes. We figured out that several factors (and their interplay) are decisive. Firstly, the ionic radii of the monovalent cations seem to affect the structure predominantly. All synthesized trivalent cation series exhibit a change in their respective space group when the monovalent cations exceed a specific size. Considering the entire lutetium series, only a single switch occurs between potassium and rubidium. The following two factors need to be treated jointly. Trivalent bismuth and antimony ions feature an s^2-configuration, so that they might express a lone pair effect where antimony is expected to have the stronger

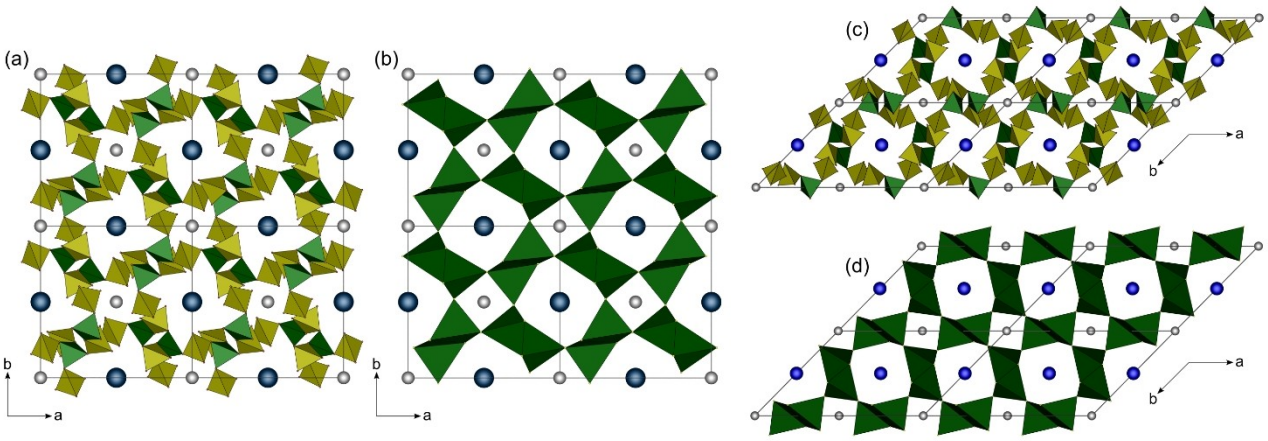

Figure 2. Crystal structures of $BiCs[B(SO_4)_2]_4$ and $SbK[B(SO_4)_2]_4$: (a) tetragonal 2x2 super cell of $BiCs[B(SO_4)_2]_4$ along [001] and (c) monoclinic 2x2 super cell of $SbK[B(SO_4)_2]_4$ along [010]; borate tetrahedra in green; sulphate tetrahedra in yellow; bismuth and antimony in grey; caesium in dark blue; potassium in blue; reduced representation of the (b) tetragonal and (d) monoclinic super cell neglecting oxygen atoms; resulting BS_4 supertetrahedra create channels of vierer and achter rings along the [001] and [010] directions, respectively.

one for electronic reasons, as discussed by Walsh and Sidgwick.[12] Here, apparently both, the ionic radii and the possible stereochemical activity, seem to be relevant. The lone pair influence can quantitatively be determined by a geometrical analysis according to the method of Balić-Žunić and Makovicky determining enclosing spheres of the coordination polyhedra, considering all ligands.[13] Accordingly, the respective centroid deviations indicate a lone pair activity.

Throughout the series, bismuth shows no stereochemical expression of the lone pair and the compounds exclusively crystallize in the tetragonal space groups $I\bar{4}$ (no. 82) and $P\bar{4}$ (no. 81); hence, the bismuth ($r^{[8]}=117$ pm) compounds behave like the lutetium compounds ($r^{[8]}=98$ pm), despite different ionic radii. In both cases the centroid deviations equal zero (Table S4). A structural comparison of $LuK[B(SO_4)_2]_4$ and $BiK[B(SO_4)_2]_4$ utilizing the program COMPSTRU[15] confirmed the strong similarity between these compounds revealing only small positional deviations (Table S6–S7). Moreover, the arithmetic means d_{av}[16] which gives a symmetry adapted average difference in the atomic position and amounts to only 0.059 Å. Therefore, these compounds can be regarded as isotypic. A large ionic radius combined with a quite rigid anion seems to be crucial for the lone pair to be quenched.

The compounds containing antimony, however, being slightly smaller than bismuth additionally adopt the monoclinic space group $C2$ (no. 5). Moreover, they show large centroid deviations depending on the combination with monovalent cations and hence express a lone pair effect (Table S4). How can we ensure that the lone pair activity drives the differing symmetry, rather than resulting from the smaller ionic radius? Lutetium and antimony, show similar ionic radii and accordingly should behave in the same fashion along the series. However, our comparison in Table 1 clearly demonstrates the structural activity of the lone pair which apparently causes the compounds to crystallize differently.

A not too special case is $Lu(Cs,H_3O)[B(SO_4)_2]_4$ where the cesium and oxonium ions are situated in the same channel but occupy two distinct sites shifted by approx. 377 pm. Cesium ions occupy only 59.6(1)% of the monovalent site, while on the remaining 40.4(1)% oxonium ions reside. Typical distances of oxonium ions to ligands resemble those of cesium ions in borosulfates[17] or cryptands.[18] Moreover, a mixed occupancy Cs/H_3O was reported for heteropolymolybdates[19] with a similar ratio.

Determining the correct space group, especially around the thresholds was challenging for some examples as the refinements in several space groups were essentially possible and provided reasonable residuals. Additional or split reflections provided evidence for the actually appropriate space group. Eventually, a careful comparison between calculated and experimental powder diffraction patterns identified the correct space group unequivocally. Hereby, $BiRb[B(SO_4)_2]_4$ and $SbK[B(SO_4)_2]_4$ serve as good examples. Both compounds were initially solved in $I\bar{4}$ with good R values but did not fit the experimental pattern sufficiently. Consequently, in both cases a symmetry reduction led to the correct determination of the space group and explained the additional reflections in the experimental pattern (Figure S1 – S2). The remaining XRD patterns of the phase pure powders are presented in the Supporting Information in Figures S6 – S8.

Furthermore, vibrational spectra were recorded. These not only showed bands typical for borate and sulfate tetrahedra but also reflect the bonding situation of the monovalent cations in their channels. Generally, the anion remains almost unchanged throughout the series despite adopting three different space groups; accordingly, only minor differences among the different compounds can be expected. Indeed, comparing the infrared spectra the fingerprint region shows no significant difference except for the regime between 1300–1400 cm^{-1} assigned to terminal S–O stretching modes. These alterations can be understood by examining the coordination situation of the monovalent cations within their channels and provide insight into the small differences among the structures. The channels are formed by terminal oxygen atoms positioned on two distinct planes and coordinate the monovalent cations (Figure 3). Depending on the cation's position, all these oxygen atoms either bind in a similar manner or exhibit two distinct binding modes which is reflected in the number of bands of the respective asymmetric stretching vibrations ν_{asym} ($S–O_{term}$). A single band is observed if all terminal oxygens contribute equally. This is the case e.g. in $BiCs[B(SO_4)_2]_4$. In contrast, two distinct bands are recorded if only oxygen atoms belonging to one on the two previously introduced planes coordinate the cation, like in e.g. $Bi(NO_2)[B(SO_4)_2]_4$. In cases where slight deviations between these two ideal scenarios occur, the bonding situation becomes more complex and hence, leads to the formation of several bands. Elusive DFT calculations on the title compounds targeting this observation are in train will be presented elsewhere.

According to thermogravimetric analyses, the bismuth and rare earth compounds behave similarly and are stable up to approximately 250 °C, whereas the antimony compounds already decompose at lower temperatures starting around 180 °C (Figure S3).[24] Consequently, the expressed lone pair effect within the antimony compounds not only has a structural influence but also decreases the thermal stability. The decomposition temperatures confirm the general trends that were observed for borosulfates so far where lower condensation degrees typically led to higher stabilities. Borosulfates solely comprising B–O–S bridges are compared in Table 2 and demonstrate this trend. Accordingly, the title compounds comprise the lowest thermal stability of this group. We assume that the significantly higher charge density on the very small sulfur cations yields a strong repulsion between adjacent sulfate moieties in condensed structures. Accordingly, less condensed borosulfate anions seem to be electrostatically, and thus thermodynamically, more favorable. Further careful studies on the thermal decomposition process including temperature programmed powder X-ray diffraction measurements are in train and will be presented elsewhere.

In this contribution we presented the very first antimony borosulfates as well as a modular system within borosulfate

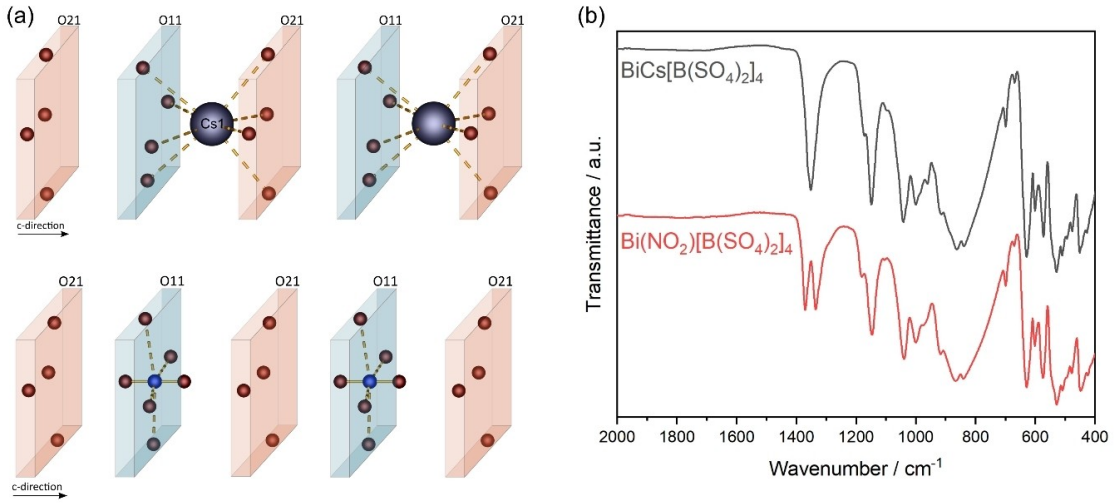

Figure 3. Position and coordination of cesium and nitronium within the one-dimensional channels in $BiCs[B(SO_4)_2]_4$ and $Bi(NO_2)[B(SO_4)_2]_4$ (left) and the respective vibrational spectra (right).

Table 2: Decomposition temperatures of reported borosulfates featuring solely B–O–S bridges in correlation with the anion's dimensionality.

Compound	T_{decomp} / °C	Dimensionality	References
$Eu_2[B_2(SO_4)_6]$	570	0 D	[7]
$Rb_5[B(SO_4)_4]$	530	0 D	[20]
$Na_5[B(SO_4)_4]$	434	0 D	[21]
$K_3[B(SO_4)_3]$	396	1 D	[21]
$Sr[B_2(SO_4)_4]$	400	1 D	[22]
$Cd[B_2(SO_4)_4]$	330	2 D	[23]
$BiRb[B(SO_4)_2]_4$	250	3 D	This work
$LuRb[B(SO_4)_2]_4$	250	3 D	This work
$SbRb[B(SO_4)_2]_4$	180	3 D	This work

chemistry $M^{III}M^{I}[B(SO_4)_2]_4$ ($M^{III} = Bi^{3+}$, Sb^{3+}, Lu^{3+}; $M^{I} = H_3O^+$, NO_2^+, Li^+, Na^+, K^+, Rb^+, Cs^+) comprising two differently charged cations. This large family of compounds crystallizes in three distinct space groups. These three, $I\bar{4}$, $P\bar{4}$ and $C2$ are related via a group-subgroup relationship. Throughout the series, this alteration in symmetry is predominantly influenced by the choice of the monovalent cation. An additional small but decisive impact is exerted by the expression of a lone pair by antimony in the respective series causing the structures to crystalize in the monoclinic space group $C2$. Moreover, the choice of the monovalent cations has an obvious influence on the pattern of vibrational bands. The thermogravimetric analyses revealed a comparably low thermal stability compared to lower dimensional borosulfates comprising solely B–O–S bridges. Complementary characterization of the compounds by DFT calculations, UV/Vis- NMR-, Mößbauer and Raman- and fluorescence spectroscopy are in train and will be presented elsewhere. Careful studies on the non-linear optical properties of these compounds are also planned.

Acknowledgements

E. T. and H. A. H. thank the Deutsche Forschungsgemeinschaft (DFG) for financial support under the project HO 4503/5. Open Access funding enabled and organized by Projekt DEAL.

Conflict of Interest

The authors declare no conflict of interest.

Data Availability Statement

The data that support the findings of this study are available in the supplementary material of this article.

Keywords: borosulfates · modular system · silicate - analogous · antimony · lutetium

[1] a) C. Martínez, A. Corma, *Coord. Chem. Rev.* **2011**, *255*, 1558; b) G. J. Hoerder, M. Seibald, D. Baumann, T. Schröder, S. Peschke, P. C. Schmid, T. Tyborski, P. Pust, I. Stoll, M. Bergler, et al., *Nat. Commun.* **2019**, *10*, 1824.
[2] A. F. Masters, T. Maschmeyer, *Micropor. Mesopor. Mater.* **2011**, *142*, 423.

[3] a) S. G. Jantz, M. Dialer, L. Bayarjargal, B. Winkler, L. van Wüllen, F. Pielnhofer, J. Brgoch, R. Weihrich, H. A. Höppe, *Adv. Opt. Mater.* **2018**, *6*; b) D. S. Wimmer, M. Seibald, D. Baumann, K. Wurst, H. Huppertz, *Chem. Eur. J.* **2023**, *29*, e202202448; c) P. Netzsch, P. Gross, H. Takahashi, S. Lotfi, J. Brgoch, H. A. Höppe, *Eur. J. Inorg. Chem.* **2019**, *2019*, 3975; d) M. Li, A. Verena-Mudring, *Cryst. Growth Des.* **2016**, *16*, 2441.
[4] a) M. Zeuner, S. Pagano, W. Schnick, *Angew. Chem.* **2011**, *123*, 7898; b) P. Netzsch, R. Stroh, F. Pielnhofer, I. Krossing, H. A. Höppe, *Angew. Chem. Int. Ed.* **2021**.
[5] J. Bruns, H. A. Höppe, M. Daub, H. Hillebrecht, H. Huppertz, *Chem. Eur. J.* **2020**, *26*, 7966.
[6] a) K. Lei, L. Xiaomeng, Z. Lin, H. Bing, *Phys. Rev. B* **2020**, *102*, 205424; b) C. Logemann, M. S. Wickleder, *Angew. Chem. Int. Ed.* **2013**, *52*, 14229; c) Z. Li, W. Jin, F. Zhang, Z. Chen, Z. Yang, S. Pan, *Angew. Chem. Int. Ed.* **2022**, *61*; d) P. Netzsch, F. Pielnhofer, H. A. Höppe, *Inorg. Chem.* **2020**, *59*, 15180; e) Z. Wang, J. Zuo, Q. Liu, X. Hou, M. Gai, *Inorg. Chem.* **2024**, *63*, 19931; f) M. D. Ward, B. L. Chaloux, M. D. Johannes, A. Epshteyn, *Adv. Mater.* **2020**, *32*, 2003667.
[7] P. Netzsch, M. Hämmer, P. Gross, H. Bariss, T. Block, L. Heletta, R. Pöttgen, J. Bruns, H. Huppertz, H. A. Höppe, *Dalton Trans.* **2019**, *48*, 4387.
[8] Y. Li, Z. Zhou, S. Zhao, F. Liang, Q. Ding, J. Sun, Z. Lin, M. Hong, J. Luo, *Angew. Chem. Int. Ed.* **2021**, *60*, 11457.
[9] a) Y. Yang, J. Wu, Y. Wang, J. Zhu, R. Liu, C. Meng, *Z. Anorg. Allg. Chem.* **2011**, *637*, 137; b) P. W. Menezes, S. Hoffmann, Y. Prots, R. Kniep, *Z. Kristallogr. - New Cryst. Struct.* **2008**, *223*, 333; c) R. Kniep, H. G. Will, I. Boy, C. Röhr, *Angew. Chem. Int. Ed.* **1997**, *36*, 1013.
[10] M. Hämmer, L. Bayarjargal, H. A. Höppe, *Angew. Chem. Int. Ed.* **2021**, *60*, 1503.
[11] Supplementary crystallographic data for the title compounds are summarized in Table S1 – S3 and may be obtained free of charge by the joint Cambridge Crystallographic Data Centre and Fachinformationszentrum Karlsruhe http://www.ccdc.cam.ac.uk/ (the International Crystallographic Structure Database (ICSD)) on quoting the CSD numbers found in the Supplements.
[12] a) A. Walsh, D. J. Payne, R. G. Egdell, G. W. Watson, *Chem. Soc. Rev.* **2011**, *40*, 4455; b) N. V. Sidgwick, *The Electronic Theory of Valency*, Oxford Clarendon Press, Oxford, **1927**.
[13] a) T. Balić Žunić, E. Makovicky, *Acta Cryst. B* **1996**, *52*, 78; b) E. Makovicky, T. Balić Žunić, *Acta Cryst. B* **1998**, *54*, 766.
[14] R. D. Shannon, *Acta Cryst. A* **1976**, *32*, 751.
[15] G. de La Flor, D. Orobengoa, E. Tasci, J. M. Perez-Mato, M. I. Aroyo, *J. Appl. Crystallogr.* **2016**, *49*, 653.
[16] D. Orobengoa, C. Capillas, M. I. Aroyo, J. M. Perez-Mato, *J. Appl. Crystallogr.* **2009**, *42*, 820.
[17] M. Daub, K. Kazmierczak, H. A. Höppe, H. Hillebrecht, *Chem. Eur. J.* **2013**, *19*, 16954.
[18] P. C. Junk, *New J. Chem.* **2008**, *32*, 762.
[19] S. Berndt, D. Herein, F. Zemlin, E. Beckmann, G. Weinberg, J. Schütze, G. Mestl, R. Schlögl, *Ber. Bunsenges. Phys. Chem.* **1998**, *102*, 763.
[20] L. Dong, S. Pan, Y. Wang, H. Yu, X. Lin, S. Han, *Mater. Res. Bull.* **2015**, *63*, 93.
[21] M. Daub, K. Kazmierczak, P. Gross, H. Höppe, H. Hillebrecht, *Inorg. Chem.* **2013**, *52*, 6011.
[22] P. Netzsch, H. A. Höppe, *Z. Anorg. Allg. Chem.* **2020**, *646*, 1563.
[23] M. Hämmer, L. C. Pasqualini, S. S. Sebastian, H. Huppertz, H. A. Höppe, J. Bruns, *Dalton Trans.* **2022**, *51*, 15458.
[24] Further thermogravimetric data is presented in the supplements Figure S4–S5.

Manuscript received: December 19, 2024
Accepted manuscript online: February 12, 2025
Version of record online: February 25, 2025